On-line Table 1: Demographic and clinical description of the study cohort of patients with oculo-auriculo-vertebral spectrum, including the presence of cranial nerve abnormalities

Patient No.		Sex	Age (yr)	Side	Involvement of				
					Ear	Face	Eye	Spine	CN
1	G	F	5	R	X	X	X		X
2	G	M	2	B	X	X	X	X	X
3	G	M	4	R	X	X		X	X
4		M	14	L	X	X			
5		F	5	R	X	X			
6		F	7	L	X	X			
7		F	4	R	X	X			
8	G	F	11	R	X	X	X		X
9	G	F	32	L	X	X	X	X	X
10	G	F	7	B	X	X	X	X	
11	G	F	8	L	X	X		X	
12	G	M	0.5	L	X	X		X	X
13		M	9	R	X	X			
14	G	M	4	L	X	X		X	
15	G	M	14	B	X	X	X	X	X
16	G	F	17	R	X	X	X	X	X
17		M	6	R	X	X			
18	G	M	6	B	X	X	X	X	X
19	G	M	4	B	X	X	X	X	X
20	G	M	8	R	X	X	X	X	X
21	G	F	3	B	X	X	X		X
22		M	5	R	X	X			
23	G	M	5	B	X	X		X	X
24	G	F	3	R	X	X	X	X	X
25	G	F	5	R	X	X	X	X	X
26	G	M	7	L	X	X	X	X	X
27		M	6	R	X	X			
28		M	8	R	X	X			
29		F	5	L	X	X			

Note:—G indicates Goldenhar phenotype (involvement of ear and hemifacial microsomia plus eye and/or spine); R, right; L, left; B, bilateral; X, present.

On-line Table 2: Features used as inclusion criteria for patients with oculo-auriculo-vertebral spectrum (auricular and hemifacial) and for characterizing the Goldenhar phenotype (concomitant vertebral and/or ocular abnormalities)

Inclusion Criteria
Auricular abnormalities
Microtia
Anotia
External acoustic canal stenosis
External acoustic canal atresia
Auricular tag
Hemifacial microsomia
Cleft lip and/or palate
Macrostomia
Malocclusion
Soft-tissue hypoplasia
Mandibular or maxillary hypoplasia
Mandibular dysplasia
Vertebral abnormalities at the cervical tract
Fusion
Deformities
Presence of hemivertebra
Ocular abnormalities
Epibulbar dermoid
Asymmetric shortening of the palpebral fissure
Microphthalmia
Anophthalmia
Coloboma
Vertical displacement of the orbit
Epicanthus

On-line Table 3: Cranial nerve and bone foramina abnormalities among patients with oculo-auriculo-vertebral spectrum

Patient No.		I		II		III		V		VI		VII		VIII		IX-XI		FO		IANC		No. of Involved CNs at MRI
		R	L	R	L	R	L	R	L	R	L	R	L	R	L	R	L	R	L	R	L	
1	G							H										A		H		1
2	G								H				H									2
3	G							F	H	A		F		F				A		A		5
4																				–	–	
5																						
6																				–	–	
7																						
8	G	–	–	A		–	–	–	–	–	–	F	F	F	F	–	–					4
9	G				H				H										A		H	1
10	G			H														–	–	–	–	
11	G									–	–	–	–		–	–	–				H	
12	G												A						H		A	1
13																						
14	G																			–	–	
15	G							F	F		A	F	F	F	–						–	6
16	G			H		H		A		A		A		A				A		H		5
17																		–	–	–	–	
18	G	–	–	–	–			F	H			F		H					H		H	4
19	G							F	H		A	F	H	A	A			–	–			7
20	G									A	A									A		2
21	G							F	H	A	A	F		F				A	A	–	–	6
22																						
23	G									A	A	F		F	A					–	–	5
24	G							H				A						–	–	–	–	2
25	G										H									–	–	1
26	G								H										H		–	1
27																				–	–	
28																		H				
29																						

Note:—FO indicates foramen ovale; IANC, inferior alveolar nerve bone canal; G, Goldenhar phenotype (involvement of ear and hemifacial microsomia plus eye and/or spine); H, hypoplasia; A, aplasia; F, fused (ie, ≥2 cranial nerves with a common origin and or course); –, not evaluable.

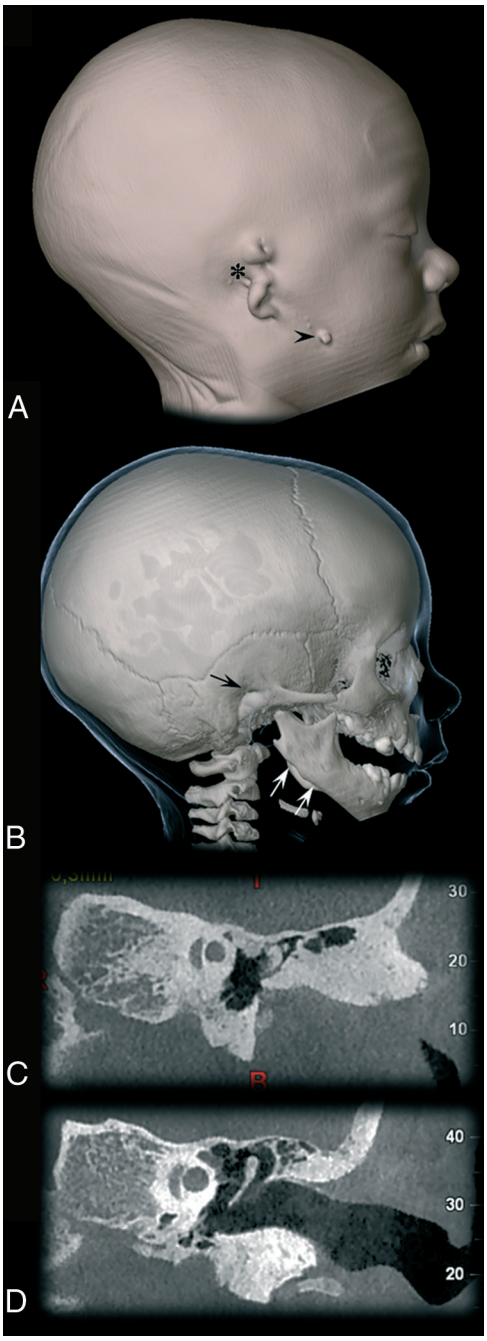

ON-LINE FIG 1. *A*, Surface-rendering technique obtained from a CT examination of a patient with oculo-auriculo-vertebral spectrum shows right microtia (*asterisk*) with a preauricular tag (*arrowhead*). *B*, 3D bone reconstruction (skin borders have been preserved) of the same patient, disclosing the external acoustic meatus atresia (*black arrow*) and hypoplasia of the ipsilateral hemimandible (*white arrows*). *C*, Conebeam CT of the same patient. Coronal multiplanar reconstruction shows the right bone atresia of the external acoustic meatus and the concomitant ossicle chain dysplasia. Note that the reconstruction is displayed in nonradiologic convention. *D*, Conebeam CT of a subject with normal ear findings presented for comparison with *C*, showing the external acoustic meatus, the ossicle chain (malleus head, neck, and part of the handle), the facial genu above and lateral to the cochlea, and the thin tendon of the tensor tympani reaching the neck of the malleus.

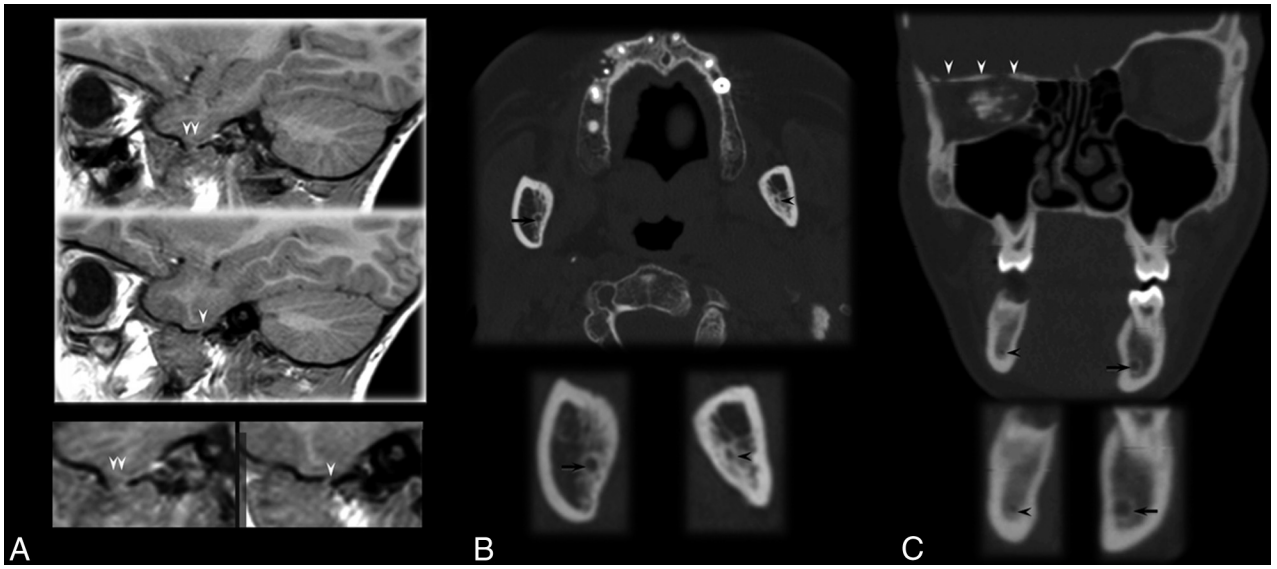

ON-LINE FIG 2. *A*, Brain MR imaging. The upper 2 images are sagittal T1-weighted images lateral to the cavernous sinuses, while the lower images are magnifications of the foramina ovalia (*arrowheads*). The latter appears as a discontinuity of the hypointense bone rim below the temporal lobe, which is easily recognizable on the left side (*double arrowheads*), while it is markedly undersized on the right side (*single arrowhead*). *B*, Head CT. The upper image is an axial image; the bone canals of the inferior alveolar nerves in the ascending branches of the mandible are asymmetric due to left hypoplasia (see also the magnifications below). *C*, Head CT. The upper image is a coronal multiplanar reconstruction displaying the marked facial asymmetry with hypoplasia of the right maxilla and hemimandible; the right orbita is particularly underdeveloped (*white arrowheads*) and a dystrophic calcified globe is recognizable; the right inferior alveolar nerve bone canal in the horizontal mandibular branch is barely identifiable due to severe hypoplasia.

ON-LINE FIG 3. Brain MR imaging. *A* and *B*, Contiguous T1-weighted axial images show the right trigeminal nerve *(arrows*) stemming from the anterior profile of the middle cerebellar peduncle; a small irregular mass (*arrowheads*) is recognizable in correspondence and slightly cranial to the origin of the cranial nerve. *C*, Sagittal T1-weighted image shows the close relationship between the nerve and the anomalous mass. Note the absence of the globe in the right orbits both in axial and sagittal images. *D*, Contiguous axial T2-weighted high-resolution images show the mass (*asterisk*) at the origin of the trigeminal nerve (*arrows*).